Membrane growth can generate a transmembrane pH gradient in fatty acid vesicles

Irene A. Chen and Jack W. Szostak*

Howard Hughes Medical Institute and Department of Molecular Biology, Massachusetts General Hospital, Boston, MA 02114

Edited by Leslie Orgel, The Salk Institute for Biological Studies, La Jolla, CA, and approved March 22, 2004 (received for review December 4, 2003)

Electrochemical proton gradients are the basis of energy transduction in modern cells, and may have played important roles in even the earliest cell-like structures. We have investigated the conditions under which pH gradients are maintained across the membranes of fatty acid vesicles, a model of early cell membranes. We show that pH gradients across such membranes decay rapidly in the presence of alkali-metal cations, but can be maintained in the absence of permeable cations. Under such conditions, when fatty acid vesicles grow through the incorporation of additional fatty acid, a transmembrane pH gradient is spontaneously generated. The formation of this pH gradient captures some of the energy released during membrane growth, but also opposes and limits further membrane area increase. The coupling of membrane growth to energy storage could have provided a growth advantage to early cells, once the membrane composition had evolved to allow the maintenance of stable pH gradients.

Modern cells rely on electrochemical proton gradients for energy transduction and metabolism. Energy obtained from light or the oxidation of organic compounds drives the generation of these gradients, which can be used as an energy source for ATP synthesis. However, these processes require complex macromolecular machinery, including membrane-bound proton pumps, which were unavailable to early cellular life. We investigated the possibility of pH gradient energy storage in fatty acid vesicles, a model system for protocellular membranes. These vesicles can take part in unusual and interesting behaviors, including autocatalytic self-assembly (1, 2) and cyclical growth and division (3). These behaviors suggest that similar self-replicating vesicles may have played a crucial role in the formation of early protocells (4–8).

In addition to their self-reproducing properties, a major advantage of fatty acid vesicles over phospholipid liposomes as prebiotic membranes is their chemical simplicity. Fatty acids have been found in extraterrestrial samples, such as the Murchison meteorite (9, 10), and can be synthesized under simulated prebiotic conditions (11–15). However, a perceived disadvantage of pure fatty acid membranes is that they are highly permeable to protons and are therefore incapable of maintaining pH gradients. Indeed, the addition of a small amount of oleic acid to phospholipid vesicles results in the dissipation of preestablished pH gradients within several seconds (16–19).

The mechanism of pH gradient decay in phospholipid vesicles doped with fatty acid is believed to involve incorporation of fatty acid into the membrane, followed by flip-flop of protonated fatty acid molecules and release of protons, thereby equilibrating the pH across the membrane (16, 20). The change of pH inside vesicles can also be used as a surrogate measurement for the change in cation concentration, in situations in which proton flux is electrically counterbalanced by cation flux (21). Cation permeability constants are quite low for model phospholipid membranes. Permeability constants for potassium through pure phosphatidylcholine membranes are typically from 10^{-10} to 10^{-12} cm/s, such that the equilibration of large unilamellar liposomes takes at least several hours (22). However, the flip-flop of fatty acids is much faster, with equilibration occurring within a few seconds (20, 23, 24).

Although previous work on proton and cation permeation has focused on pure phospholipid membranes or phospholipid membranes doped with a small amount of fatty acid, fatty acids themselves form negatively charged vesicles when prepared at a pH close to the pK_a of the acid when incorporated into the membrane (25–27). Vesicles are initially formed as an aqueous dispersion of fatty acid, with a highly polydisperse size distribution (50 nm to several microns in diameter; ref. 28), which is consistent with the thermodynamics of vesicle systems (29). These preparations can be extruded through small-pore filters to yield vesicles of a defined size (30) that are stable for at least several hours (3, 25). Under these conditions, fatty acid micelles and free molecules are present in equilibrium with vesicles at a concentration equal to the critical aggregate concentration (cac), which is similar to a phase equilibrium (1, 31).

For pure fatty acid vesicles prepared in high buffer concentrations, proton flux driven by a transmembrane pH gradient would soon lead to a significant membrane potential, halting further flux unless cations were moved in the opposite direction (21, 32). To understand the properties of pure fatty acid vesicles with respect to the maintenance and decay of pH gradients, we studied the pathway of proton flux and found that the transmembrane movement of cation-associated fatty acid appears to be the rate determining process in pH gradient decay. We also used an impermeant cation, arginine, to create pure fatty acid vesicles that can maintain a pH gradient for several hours.

The ability of fatty acid vesicles to grow by incorporating additional fatty acid is one of their most interesting dynamic properties from an origin-of-life perspective. Growth can be achieved by the addition of fatty acid micelles, prepared at high pH, to a solution of preformed vesicles buffered at the proper pH. The system is transiently out of equilibrium upon micelle addition but reequilibrates as the fatty acid is incorporated into preformed and *de novo* vesicles (33). The final vesicle size distribution may depend on the protocol used for micelle addition (2, 3, 28). Growth in these systems has been demonstrated by several methods, including cryotransmission electron microscopy (2), dynamic light scattering (DLS) (34, 35), field flow fractionation with inline multiangle light scattering, and fluorescence resonance energy transfer (FRET) changes in membrane-incorporated dyes (3). The FRET assay relies on the distance-dependent fluorescence of nonexchanging lipid dyes. As membrane area increases, the surface density of the dyes decreases, causing a quantitative decrease in the FRET signal. This assay has been used to specifically measure changes in the surface area of preformed membranes, and it is insensitive to the potentially confounding effects of *de novo* vesicle formation and the so-called "matrix effect" on vesicle diameter (28).

In fatty acid vesicles capable of maintaining a pH gradient, we found that growth resulted in the creation of a pH gradient,

This paper was submitted directly (Track II) to the PNAS office.

Abbreviations: DLS, dynamic light scattering; FRET, fluorescence resonance energy transfer; HPTS, 8-hydroxypyrene-1,3,6-trisulfonic acid; cac, critical aggregate concentration.

*To whom correspondence should be addressed. E-mail: szostak@molbio.mgh.harvard.edu.

BIOPHYSICS

because protonated fatty acid molecules crossed the membrane and released protons into the interior. Our results demonstrate a simple means of capturing some of the energy released during membrane growth. Our results also put strong constraints on the composition of a protocellular system capable of maintaining and using pH gradients.

Materials and Methods

Materials. Oleic (C18:1), palmitoleic (C16:1), and myristoleic (C14:1) acid, and monomyristolein (the glycerol ester of myristoleic acid) were purchased from Nu Chek Prep (Elysian, MN). A quantity of 1-palmitoyl-2-oleoyl-sn-glycero-3-phosphocholine (POPC) was purchased from Avanti Polar Lipids; 8-hydroxypyrene-1,3,6-trisulfonic acid (HPTS; pyranine), *N*-(7-nitrobenz-2-oxa-1,3-diazol-4-yl)-1,2-dihexadecanoyl-*sn*-glycero-3-phosphoethanolamine (NBD-PE), and lissamine rhodamine B 1,2-dihexadecanoyl-*sn*-glycero-3-phosphoethanolamine (Rh-DHPE) were purchased from Molecular Probes; and ^{3}H-arginine was purchased from New England Nuclear. All other chemicals were purchased from Sigma-Aldrich (St. Louis).

Preparation of Fatty Acid Vesicles. Large unilamellar vesicles were prepared by mixing fatty acid with buffer (0.2 M bicine unless otherwise noted) to obtain the desired pH, typically between 7 and 9. To encapsulate HPTS, 0.5 mM HPTS was included in the resuspension solution. Vesicles labeled with the FRET dyes *N*-(7-nitrobenz-2-oxa-1,3-diazol-4-yl)-1,2-dihexadecanoyl-*sn*-glycero-3-phosphoethanolamine (NBD-PE) and lissamine rhodamine B 1,2-dihexadecanoyl-*sn*-glycero-3-phosphoethanolamine (Rh-DHPE) were prepared by mixing the dyes with fatty acid in methanol, removing the solvent by rotary evaporation, and resuspending in the desired buffer. The pH of buffer solutions was adjusted with the appropriate cation hydroxide. Final fatty acid concentration in the preparation was 80 mM. Preparations were vortexed briefly and mixed end over end overnight under argon. Vesicles were extruded for eleven passes through 100-nm pore filters by using the MiniExtruder system (Avanti Polar Lipids), unless otherwise noted. Vesicles were purified from unencapsulated dye by using a gravity-flow size exclusion column (Sepharose 4B). Myristoleic acid/monomyristolein vesicles were prepared by mixing 0.5 equivalents of neat monomyristolein with fatty acid, and then following the above procedure.

Fatty Acid Micelles. Fatty acid micelles were prepared by using alkali hydroxide as described (3). For stock solutions of oleate-arginine micelles, neat fatty acid was added to a 13–15% methanol solution containing one equivalent of arginine. This addition was necessary because micelles prepared without methanol formed a gel. The final concentration of methanol in growth reactions was <0.6%. This amount did not affect HPTS fluorescence or cause detectable leakage of encapsulated dye. DLS of oleate-arginine micelles was measured by an ALV/DLS/SLS-5000 compact goniometer system (ALV-GmbH, Langen, Germany) with a CW argon-ion laser and a detection angle of 90°. Data were analyzed by the method of cumulants (36, 37).

pH Measurement. A pH meter (pH-25, Corning) was used to determine the pH of buffer solutions and vesicle solutions during preparation. Encapsulated HPTS was used to monitor internal vesicle pH. HPTS was excited at 402 and 460 nm and the emission was detected at 510 nm. The ratio of these emissions depends on the pH (38), and a standard curve was made by using vesicles prepared at different pH. All fluorescence measurements were performed by using a Cary Eclipse fluorimeter (Varian).

Assay for Surface Area Growth in Vesicles. FRET efficiencies (ε) were approximated as $1 - F_v/F_t$, where F_v is donor fluorescence in vesicles and F_t is donor fluorescence after the addition of 1% Triton X-100 (39, 40). Donor fluorescence was measured at 530 nm with excitation at 430 nm. A standard curve was generated by using known dye concentrations in vesicles.

Stopped-Flow Kinetics. Vesicles were diluted to a concentration between 1.5 and 6 mM and were loaded into a 2.5-ml syringe of the RX-2000 rapid mix accessory to the fluorimeter (Applied Photophysics, Surrey, U.K.). In pH gradient decay experiments, buffer of the appropriate pH was loaded into a 2.5-ml syringe. The observed rate constant (k) of pH gradient decay was used to calculate a permeability coefficient by using the formula $P = k(V/S)$, where V and S are the calculated volume and surface area of a 100-nm diameter vesicle, respectively. In growth experiments, micelles were loaded into a 100-μl syringe in 25-fold excess of the desired final concentration. Stopped-flow mixing was performed according to manufacturer's instructions. Fluorescence data were converted to internal vesicle pH or relative surface area by using the standard curves. Time course curves were fit to first-order exponential decay equations by using nonlinear regression.

Arginine Permeability Assay. A quantity of ^{3}H-arginine (2 μCi; 1 Ci = 37 GBq) was encapsulated by addition to buffer before resuspension with oleic acid. Vesicles were purified from unencapsulated ^{3}H-arginine by size exclusion chromatography (Sepharose 4B). Size exclusion chromatography was repeated at different time points and the radioactivity in encapsulated and unencapsulated fractions was quantified by scintillation counting.

Determination of Cac. Oleate vesicles were prepared by diluting a micelle stock into 0.2 M bicine, pH 8.5. After mixing for 3 h, the turbid solution was serially diluted in the concentration range from 1 μM to 2 mM. The 90° light scattering was measured by a PDDLS/Batch system (Precision Detectors, Bellingham, MA). Scattering intensities at low and high concentrations were log-transformed and were fit to straight lines, and the point of intersection was used to estimate the cac.

Results

We first verified that fatty acid vesicles prepared in the presence of alkali metal cations show high proton permeability. Vesicles prepared in 0.2 M bicine, pH 8.5 by using Na^+, K^+, Cs^+, or Rb^+ as a cation were mixed with buffer in a stopped-flow device to a final pH of 8.0, thereby establishing a pH gradient across the membrane. The internal pH of the vesicles was calculated from the changes in the fluorescence of an encapsulated dye, HPTS. pH equilibration occurred within a few seconds and data were well fit by a single exponential decay (Fig. 1*A*). Macroscopic membrane defects were ruled out as a cause of equilibration by checking for dye leakage by size exclusion chromatography after mixing. Also, oleate-K^+ vesicles prepared by extrusion to 400 nm, which results in a heterogeneous population of vesicles with diameters of <400 nm, equilibrated more slowly than 100-nm extruded vesicles, as expected from the smaller surface-area-to-volume ratio. Furthermore, the addition of monomyristolein (41), a nonionizable membrane component, to myristoleate vesicles reduced the rate of pH gradient decay, also suggesting that the fatty acid mediates proton transport (Table 1). As a control, 1-palmitoyl-2-oleoyl-sn-glycero-3-phosphocholine liposomes were shown to maintain an internal pH at 8.5 under the same mixing conditions, in agreement with previous work (20, 47), and no fluorescence changes were observed when fatty acid vesicles were mixed with buffer at pH 8.5.

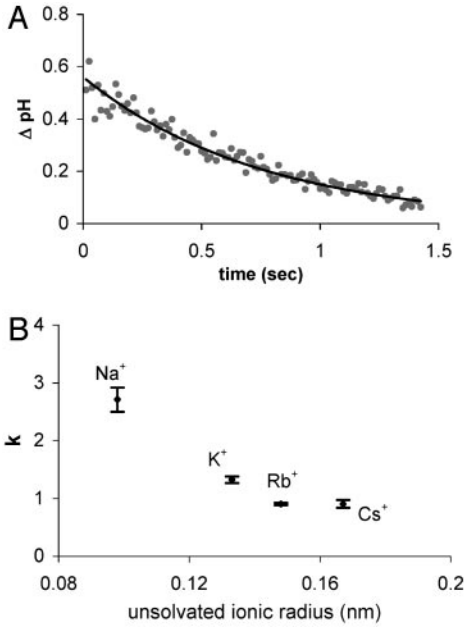

Fig. 1. pH gradient decay in oleate vesicles prepared with alkali metal cations. (*A*) Time course of pH gradient decay for oleate vesicles prepared with K^+-bicine at pH 8.5, diluted to pH 8. The line is an exponential fit to: $\Delta pH = 0.56e^{-1.32\,t}$; $r^2 = 0.95$. (*B*) Plot of first-order rate constant *k* of pH gradient decay in vesicles vs. unsolvated ionic radius; the radius reflects the strength of coulombic attraction at the inner Helmholtz plane of the membrane (44–46). Error bars are SD from replicates.

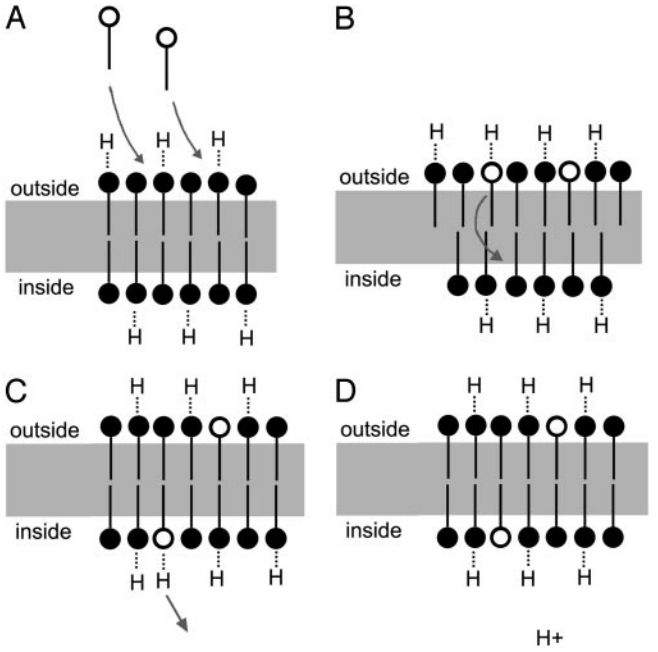

Fig. 2. Model of growth resulting in acidification of the vesicle interior. (*A*) Fatty acid is added to the exterior of the vesicle to initiate growth. Near the pK_a of fatty acid in the membrane, roughly half are protonated and half are negatively charged. Negative charges are not shown for clarity. (*B*) Fatty acid is incorporated into the outer leaflet of the vesicle bilayer. (*C*) Approximately half of the incorporated fatty acid flip-flops into the inner leaflet to maintain mass balance. Because the fatty acid is electrically neutral when protonated, the protonated form is preferentially transferred through the hydrophobic membrane. (*D*) Inside the vesicle, the fatty acid equilibrates to the pH of the solution, i.e., approximately half of the transferred fatty acid releases a proton into solution inside the vesicle. In order for these events to result in overall acidification of the vesicle interior, the membrane must be relatively impermeable to other cations in solution.

Due to the high buffer concentration, the observed proton flux was too large to result from unidirectional fatty acid flip-flop and ionization. Because the membrane is only very slowly permeable to bicine (42), the fast pH gradient decay must be mediated by cation flux balancing proton flux (43). The rate constant of decay (*k*) for alkali metals decreased moderately when proceeding down the periodic table (Fig. 1*B*). These rate constants translate into cation permeability coefficients on the order of 10^{-6} cm/s, which is much higher than permeability coefficients of pure phospholipid membranes, as expected. This result is also higher than the observed permeability of phospholipid membranes doped with small amounts of fatty acid, in which ionized oleate flip-flops slowly, for which the effective permeability of the oleate fraction of the membrane would be $<10^{-8}$ cm/s for large proton fluxes (20).

Our data for pure fatty acid vesicles are consistent with a mode of cation transport analogous to proton transport by fatty acid flip-flop, in which anionic oleate acts as an ionophore (47). To test this hypothesis, we prepared membranes composed of fatty acids with shorter acyl chains, which should exhibit faster flip-flop and therefore faster cation transport. This finding was verified by using myristoleate and palmitoleate vesicles prepared with K^+ (Table 1). This transport pathway avoids the electrostatic barrier to transport of ions by diffusion through the hydrophobic core (48), and it allows fast cation permeation through fatty acid vesicles, relative to model membranes composed of phospholipids, which have flip-flop lifetimes of several hours (49).

Table 1. Vesicle size, chain length, and the rate constant of pH gradient decay

Fatty acid	Chain length	Extrusion size, nm	$k \pm 2\sigma$, s^{-1}
Oleic	18	400	0.74 ± 0.08
		100	1.32 ± 0.12
Palmitoleic	16	100	2.4 ± 0.5*
Myristoleic	14	100	2.7 ± 0.3*
Myristoleic/monomyristolein (2:1)	14	100	0.4 ± 0.1*

*These rate constants were adjusted to account for the smaller size of these extruded vesicles, as determined by DLS (3, 33).

We were initially motivated to study the decay of pH gradients in pure fatty acid vesicles because we predicted that vesicle growth would generate a pH gradient. Growth should acidify the vesicle interior because half of the fatty acid that is initially incorporated into the outer leaflet of the membrane must transfer to the inner leaflet. This action presumably occurs through the flip-flop of the protonated acid, which is much faster than the flip-flop of negatively charged oleate (50). Fatty acid added to the inner leaflet would then equilibrate with the vesicle interior, causing acidification (20). This process would store some of the energy released during spontaneous vesicle growth in the form of a pH gradient (Fig. 2).

To test this hypothesis, we required a fatty acid vesicle system that could maintain a pH gradient. Because cation permeability appeared to determine the rate of pH gradient decay across fatty acid membranes, we looked for chemically simple but impermeant cations to prevent the decay of pH gradients. Choline, which has been used to prevent cation flux in phospholipid membranes (32), slowed pH gradient decay somewhat ($t_{1/2} \approx 6$ sec) in oleate vesicles. Arginine slowed the decay to a time scale much longer than growth ($t_{1/2} \approx 16$ h, Fig. 3*A*), which agreed with the observed arginine permeability time scale. As expected, no

BIOPHYSICS

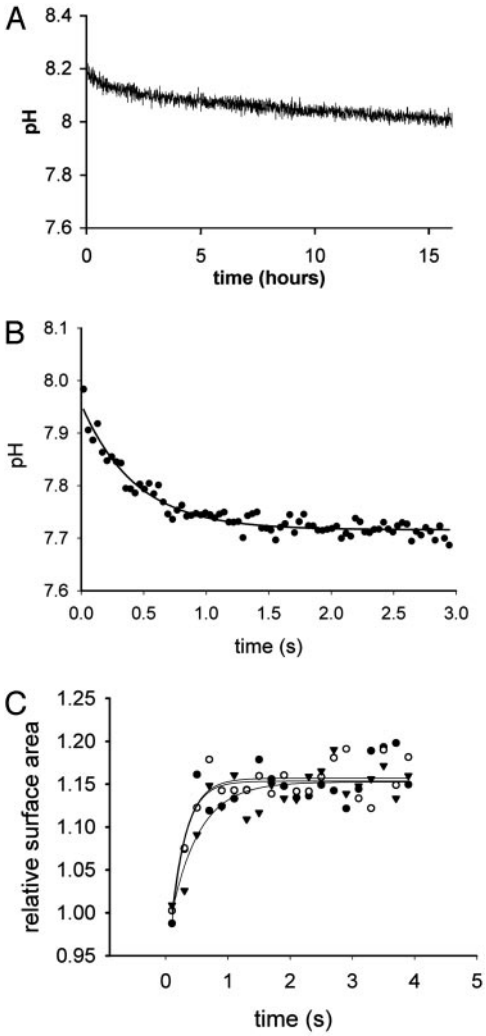

Fig. 3. Acidification during growth of oleate-arginine vesicles. (*A*) Vesicles prepared at pH 8.2 were diluted to a final pH of 7.7. Oleate-arginine vesicles were observed to have a range of pH stability ≈0.3 pH units lower than vesicles prepared with alkali ions. The fast initial drop of ≈0.06 pH units may be due to trace amounts of metal cations or other impurities. (*B*) Typical pH drop observed during growth after addition of one equivalent of oleate micelles. In this case, the vesicle interior and exterior were initially buffered at pH 8.0 with 0.2 M arginine-bicine. The line is an exponential decay curve; parameters are given in Table 2. (*C*) Relative surface area of vesicles during growth, after adding one equivalent of oleate micelles. Initially, the interior pH of these vesicles was 8.1 and the exterior pH was 7.2. Three trials are shown, and each line represents a single exponential curve fit. Average growth = 15%; average rate constant = 3.7 s^{-1}.

fluorescence changes were observed when oleate-arginine vesicles were mixed with buffer prepared at the same pH. Oleate-arginine micelles were examined by DLS, which indicated an average hydrodynamic radius of 1.8 nm, compared with 1.3 nm for Na^+-oleate micelles.

With the oleate-arginine system, we were able to study whether membrane growth caused pH acidification inside vesicles. Oleate-arginine vesicles were grown by stopped flow mixing of one equivalent of micelles with buffered vesicles. A significant internal pH drop was in fact observed upon micelle addition (Fig. 3*B* and Table 2). No change in fluorescence was observed when vesicles were mixed with a control solution of arginine and methanol in water. However, an increase in surface area could not be detected by the FRET assay, suggesting that

Table 2. pH drop in oleate-arginine vesicles during growth

Buffer concentration	External pH	Internal pH: Before growth	Internal pH: After growth	$k \pm 2\sigma$, s^{-1}
50 mM	8.0	8.0	7.76 ± 0.01	3.6 ± 0.4
0.2 M	8.0	8.0	7.73 ± 0.04	2.6 ± 1.2
0.2 M	7.2	8.1	7.34 ± 0.04	5.1 ± 0.6
0.2 M	7.7	8.1	7.62 ± 0.004	2.0 ± 0.2
0.2 M*	7.7	—	7.54 ± 0.01	3.2 ± 2.2

*A second equivalent of micelles was added to vesicles obtained from the reaction of the preceding line.

the amount of growth was smaller than the detection limit (≈7%). For comparison, oleate-Na^+ vesicles show an ≈70% surface area increase under similar growth conditions. We therefore tested whether oleate-arginine vesicles were for some reason only capable of incorporating a small amount of fatty acid. At a lower buffer concentration, a fixed amount of growth should translate into a larger internal pH drop due to the decreased buffering capacity. However, the same pH drop (≈0.3 units) was observed at low (50 mM) and high (0.2 M) bicine buffer concentrations. We also verified that oleate-arginine vesicles are stable over the pH range explored (pH 7.1–8.3), as shown by size exclusion chromatography of encapsulated HPTS, indicating that acidification did not cause gross destabilization of the membrane.

An intriguing possibility was that the pH gradient itself opposed further growth. As a pH gradient develops across the membrane, it becomes increasingly difficult to further increase the pH gradient because work must be performed against the gradient (51). The magnitude of the additional work would not depend on the buffer concentration, which is consistent with the results described above. We hypothesized that a preexisting but opposite pH gradient, i.e., vesicle interior alkaline relative to the external buffer, would allow a greater decrease in internal pH during growth. Indeed, if vesicles were prepared at high pH, diluted into a lower pH buffer, and then mixed with micelles, the magnitude of internal acidification increased as the pH of the exterior buffer decreased, causing a pH drop of up to 0.8 pH units (Table 2). Although the surface area increase of oleate-arginine vesicles had been undetectable by the FRET assay when the initial internal and external pHs were equal, membrane growth of these initially alkaline vesicles was detectable as a 15% increase in surface area. Moreover, the increase observed by FRET had a time scale identical to the time scale of the acidification. (Fig. 3*C*).

In a further search for factors that could limit the growth of oleate-arginine vesicles, we asked whether the state of the added micelles could influence the extent of fatty acid incorporation into preformed membranes. Micelles diluted into an intermediate pH are rapidly transformed into metastable structures, which slowly evolve into vesicles (33). Because the energetically favorable micelle-to-vesicle transition drives growth, the driving force for growth decreases as the micelles are gradually altered in the low pH environment. We hypothesized that if a second aliquot of freshly prepared micelles was added to vesicles that had been previously grown to equilibrium, further vesicle growth should occur. As predicted, further acidification was observed upon addition of fresh micelles (Table 2). Taken together, these results indicate that vesicle growth was not limited by intrinsic properties of the membrane, but rather that growth stops when the "back pressure" of the proton gradient equals the driving force for growth (52, 53).

Discussion

The observed fast pH gradient decay in pure fatty acid vesicles prepared with alkali metal cations extends previous observations of rapid proton permeability mediated by small amounts of oleic acid (<5 mol %) in phospholipid vesicles (20, 51, 54). We found that the rate of pH gradient decay depends strongly on the identity of the cation, such that a relatively impermeant cation, arginine, allowed pH gradients to be maintained for several hours. This result is consistent with electroneutrality requirements, because uncompensated directional proton movement would create a transmembrane potential, limiting further ion flux.

We determined the rate of decay of a pH gradient in the presence of different alkali metal cations. Because large changes in proton concentration were necessary to change the pH of the buffered solution in these experiments, proton flux was effectively limited by cation flux in the opposite direction. The decay of the pH gradient was therefore an indirect measure of the simultaneous decay of the cation gradient. Na^+ was found to be most permeable, followed by K^+, and Rb^+, and Cs^+ (Fig. 1*B*). Alkali metal cations were more permeant to fatty acid vesicles than to phospholipid vesicles by several orders of magnitude. These data are consistent with a pathway in which oleate acts as an ionophore associating with alkali metal ions (47). The affinities of the alkali metal cations for negatively charged phospholipid liposomes follow the trend $Na^+ > K^+ > Rb^+ > Cs^+$ (55–57). A higher affinity of Na^+ for the fatty acid membrane may result in a greater effective concentration of the cation-ionophore pair, leading to faster cation permeation.

The pathway for cation transport may be written as follows, where subscripts *i* and *o* on chemical species denote the volumes on the inside and outside of the vesicle respectively, C^+ denotes a cation, and FA^- denotes a deprotonated fatty acid (e.g., oleate).

$$C_i^+ + FA_i^- \underset{k_{-1}}{\overset{k_1}{\rightleftharpoons}} \{C{-}FA\}_i \overset{k_2}{\longrightarrow} \{C{-}FA\}_o \underset{k_{-3}}{\overset{k_3}{\rightleftharpoons}} C_o^+ + FA_o^-$$

Assuming that pH gradient decay is limited by cation transport, the apparent rate constant (k_{app}) for pH gradient decay is $(k_1/k_{-1})\ k_2\ [FA_i^-]$. k_1/k_{-1} is the association constant of cation and fatty acid, which is affected by the identity of the cation. The fatty acid chain length affects k_2, because short chains should allow faster flip-flop, as observed. This mechanism maintains mass balance of the inner and outer leaflets during pH gradient decay, avoiding the need to invoke transmembrane movement of charged oleate anions. Because the concentration of ionized fatty acid on the inner leaflet, $[FA_i^-]$, is itself a function of the internal pH, k_{app} may be expected to change during the course of pH gradient decay. Our failure to observe a significant departure from single-exponential decay of the pH gradient may simply reflect the noise in our experimental data, but could also reflect a degree of cooperativity in the ionization of lamellar phase fatty acid, which would limit changes in $[FA_i^-]$ over the measured pH range (27).

We studied the generation of a transmembrane pH gradient during growth by using oleate-arginine vesicles (Fig. 2), because pH gradients across oleate-arginine vesicles did not decay significantly on the experimental time scale. We observed the expected acidification of vesicle interiors upon addition of oleate micelles to preformed vesicles, but the surface area increase of oleate-arginine vesicles was significantly less than that of oleate-Na^+ vesicles. The pH drop itself limited further gradient formation, and when an opposing pH gradient was experimentally imposed, we were able to significantly increase the magnitude of the pH drop. By using an assay based on FRET between two lipid-incorporated probes, we verified that an increase in vesicle surface area (i.e., membrane growth) occurs simultaneously with and at the same rate as the pH drop.

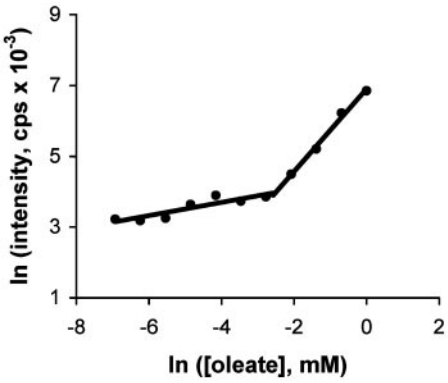

Fig. 4. Determination of the cac by 90° static light scattering. ln(photon intensity) vs. ln(concentration of oleate) in 0.2 M bicine, pH 8.5. Straight lines were fit to the low-concentration micelle regime and high-concentration vesicle regime. The point of intersection was used to estimate the cac (82 μM).

The conversion of micelles to vesicles is exergonic, and some of this energy was transduced into a transmembrane pH gradient. To estimate the efficiency of this conversion, the free energy of the micelle to vesicle transition was estimated from the cac of oleic acid in our system (82 μM, Fig. 4), by using a phase transition model for micelle-vesicle equilibrium at large aggregation numbers. The standard free energy released per mole of oleate converted from micelles to vesicles is given by $\Delta G^\circ_{transition} = 1.5\,RT\ln(cac)$, in which the cac is given in units of mol fraction (58, 59). The factor of 1.5 is an adjustment for the difference in the degree of ionization between micelles and vesicles, assuming that one-half equivalent of cations is released during the transition from micelles to vesicles (31). For the addition of 1.5 mM micelles, $\Delta G_{transition} = -11$ kJ/mol. Given the size of the vesicle (100 nm diameter) and the approximate amount of growth, we estimated that 1.9×10^{-16} J are released per vesicle during growth.

The energy stored in a 0.3-pH unit transmembrane gradient per mol of protons transferred is given by $\Delta G_{gradient} = -2.3\,RT(\Delta pH) = -1.7$ kJ/mol. The titration of 0.2 M bicine from pH 8 to 7.7 requires the addition of 25 mM H^+. Given the volume of a vesicle, 2.2×10^{-17} J are stored in the pH gradient per vesicle. Thus, the overall efficiency of energy transfer from the micelle to vesicle transition into the pH gradient was ≈12%.

Part of this energetic loss is a necessary consequence of the process of growth. Approximately half of the fatty acid molecules incorporated into a preformed vesicle will be incorporated into the inner leaflet. Of these, approximately half will dissociate to produce a proton and the corresponding anion, because the solution is near the pK_a of the membrane-incorporated fatty acid. Given these losses, the theoretical maximum efficiency for the conversion of energy into the pH gradient would be 25%. The remainder of the energy loss may be due to several factors, including the fast relaxation of micelles into metastable structures and entropic increases resulting from alterations in the structure of water surrounding the micelle or vesicle. The observed energy efficiency is similar to that of other energy transduction systems based on pH gradients (52); for example, the energy efficiency of photosynthetic conversion of absorbed red light into reduced carbon is 34% (60). In comparison with these systems, however, energy transduction is achieved in oleate-arginine vesicles with only a few chemical components, namely oleate and a buffer by using an impermeant cation.

BIOPHYSICS

This simple chemical system demonstrates energy storage in the form of a pH gradient created by spontaneous vesicle growth. In a prebiotic context, growing vesicles might gain a selective advantage if the gradient could be used to drive other useful processes, such as uptake of metabolically useful amines (61). From a systems perspective, this process may couple growth of one protocellular component, the membrane, to the growth of other components that are able to use the stored energy. These studies also emphasize that the maintenance of a substantial transmembrane pH gradient in fatty acid vesicles is contingent on a membrane with low cation permeability. To use the energy released during membrane growth, early protocells using fatty acid membranes would have had to exist in the absence of a substantial concentration of alkali cations, which seems unlikely. Therefore, the ability to use energy stored in pH gradients may not have been possible until the evolution of membranes composed of less permeable membrane components, such as phosphate or glycerol esters, and with relatively low steady-state levels of free fatty acids.

Finally, our observation that the development of an internally acidic pH gradient is strongly inhibitory to further membrane growth suggests that the evolution of less permeable membranes may have required the coevolution of ionophores to relax the inhibitory pH gradient. Further advantage may have been obtained through the evolution of a proton "pump," requiring energetic input, that could generate an alkaline vesicle interior to increase the rate of membrane growth (61, 62). Such a pump, running in reverse, could have been co-opted later as part of a mechanism to couple a transmembrane gradient to the formation of energy-rich bonds.

We thank Shelly Fujikawa, Martin Hanczyc, and Pierre-Alain Monnard for technical advice and comments on the manuscript; Johan Mattson and David Weitz for guidance and use of the ALV-DLS; and David Deamer, Matthew Hartman, and Ching-Hsuan Tsai for comments on the manuscript. J.W.S. is an investigator of the Howard Hughes Medical Institute. This work was supported in part by National Aeronautics and Space Administration Exobiology Program Grant EXB02-0031-0018; National Institutes of Health Medical Scientist Training Program Grant T32-GM07753 (to I.A.C.); and National Institutes of Health Molecular Biophysics Training Grant T32-GM08313 (to I.A.C.).

1. Walde, P., Wick, R., Fresta, M., Mangone, A. & Luisi, P. L. (1994) *J. Am. Chem. Soc.* **116,** 11649–11654.
2. Berclaz, N., Muller, M., Walde, P. & Luisi, P. L. (2001) *J. Phys. Chem. B* **105,** 1056–1064.
3. Hanczyc, M. M., Fujikawa, S. M. & Szostak, J. W. (2003) *Science* **302,** 618–622.
4. Szathmary, E. & Demeter, L. (1987) *J. Theor. Biol.* **128,** 463–486.
5. Chakrabarti, A. C., Breaker, R. R., Joyce, G. F. & Deamer, D. W. (1994) *J. Mol. Evol.* **39,** 555–559.
6. Cavalier-Smith, T. (2001) *J. Mol. Evol.* **53,** 555–595.
7. Segre, D., Ben-Eli, D., Deamer, D. W. & Lancet, D. (2001) *Origins Life Evol. Biosphere* **31,** 119–145.
8. Szostak, J. W., Bartel, D. P. & Luisi, P. L. (2001) *Nature* **409,** 387–390.
9. Yuen, G. U. & Kvenvolden, K. A. (1973) *Nature* **246,** 301–303.
10. Deamer, D. W. (1985) *Nature* **317,** 792–794.
11. Allen, W. V. & Ponnamperuma, C. (1967) *Curr. Mod. Biol.* **1,** 24–28.
12. Yuen, G. U., Lawless, J. G. & Edelson, E. H. (1981) *J. Mol. Evol.* **17,** 43–47.
13. McCollom, T. M., Ritter, G. & Simoneit, B. R. (1999) *Origins Life Evol. Biosphere* **29,** 153–166.
14. Rushdi, A. I. & Simoneit, B. R. (2001) *Origins Life Evol. Biosphere* **31,** 103–118.
15. Dworkin, J., Deamer, D., Sandford, S. & Allamandola, L. (2001) *Proc. Natl. Acad. Sci. USA* **98,** 815–819.
16. Gutknecht, J. (1988) *J. Membr. Biol.* **106,** 83–93.
17. Schonfeld, P., Schild, L. & Kunz, W. (1989) *Biochim. Biophys. Acta* **977,** 266–272.
18. Zhang, F., Kamp, F. & Hamilton, J. A. (1996) *Biochemistry* **35,** 16055–16060.
19. Pohl, E. E., Peterson, U., Sun, J. & Pohl, P. (2000) *Biochemistry* **39,** 1834–1839.
20. Kamp, F. & Hamilton, J. A. (1992) *Proc. Natl. Acad. Sci. USA* **89,** 11367–11370.
21. Deamer, D. W. & Nichols, J. W. (1983) *Proc. Natl. Acad. Sci. USA* **80,** 165–168.
22. Paula, S., Volkov, A. G., Van Hoek, A. N., Haines, T. H. & Deamer, D. W. (1996) *Biophys. J.* **70,** 339–348.
23. Kamp, F., Zakim, D., Zhang, F., Noy, N. & Hamilton, J. A. (1995) *Biochemistry* **34,** 11928–11937.
24. Kleinfeld, A. M., Chu, P. & Romero, C. (1997) *Biochemistry* **36,** 14146–14158.
25. Gebicki, J. M. & Hicks, M. (1973) *Nature* **243,** 232–234.
26. Small, D. M. (1986) in *The Physical Chemistry of Lipids: From Alkanes to Phospholipids*, ed. Small, D. M. (Plenum, New York), pp. 285–343.
27. Cistola, D. P., Hamilton, J. A., Jackson, D. & Small, D. M. (1988) *Biochemistry* **27,** 1881–1888.
28. Blochliger, E., Blocher, M., Walde, P. & Luisi, P. L. (1998) *J. Phys. Chem. B* **102,** 10383–10390.
29. Israelachvili, J. N. (1991) *Intermolecular and Surface Forces* (Academic, London).
30. Hope, M. J., Bally, M. B., Webb, G. & Cullis, P. R. (1985) *Biochim. Biophys. Acta* **812,** 55–65.
31. Blandamer, M. J., Cullis, P. M., Soldi, L. G., Engberts, J. B., Kacperska, A., Van Os, N. M. & Subha, M. C. (1995) *Adv. Colloid Interface Sci.* **58,** 171–209.
32. Nichols, J. W. & Deamer, D. W. (1980) *Proc. Natl. Acad. Sci. USA* **77,** 2038–2042.
33. Chen, I. & Szostak, J. W. *Biophys. J.*, in press.
34. Lonchin, S., Luisi, P. L., Walde, P. & Robinson, B. H. (1999) *J. Phys. Chem. B* **103,** 10910–10916.
35. Rasi, S., Mavelli, F. & Luisi, P. L. (2003) *J. Phys. Chem. B* **107,** 14068–14076.
36. Koppel, D. E. (1972) *J. Chem. Phys.* **57,** 4814–4820.
37. Frisken, B. J. (2001) *Appl. Opt.* **40,** 4087–4091.
38. Kano, K. & Fendler, J. H. (1978) *Biochim. Biophys. Acta* **509,** 289–299.
39. Fung, B. K.-K. & Stryer, L. (1978) *Biochemistry* **17,** 5241–5248.
40. Struck, D. K., Hoekstra, D. & Pagano, R. E. (1981) *Biochemistry* **20,** 4093–4099.
41. Monnard, P. A. & Deamer, D. W. (2003) *Methods Enzymol.* **372,** 133–151.
42. Fujikawa, S. M. (2003) Ph.D. thesis (Harvard Univ., Boston).
43. Venema, K., Gibrat, R., Grouzis, J. P. & Grignon, C. (1993) *Biochim. Biophys. Acta* **1146,** 87–96.
44. Grahame, D. C. (1947) *Chem. Rev. (Washington, D.C.)* **41,** 441–501.
45. Plesner, I. W. & Michaeli, I. (1974) *J. Chem. Phys.* **60,** 3016–3024.
46. Hunter, R. J. (2001) *Foundations of Colloid Science* (Oxford Univ. Press, Oxford).
47. Zeng, Y., Han, X., Schlesinger, P. & Gross, R. W. (1998) *Biochemistry* **37,** 9497–9508.
48. Volkov, A. G., Paula, S. & Deamer, D. W. (1997) *Bioelectrochem. Bioenerg.* **42,** 153–160.
49. van der Meer, B. W. (1993) in *Biomembranes: Physical Aspects*, ed. Shinitzky, M. (VCH, New York), pp. 97–158.
50. Hamilton, J. A. (1998) *J. Lipid Res.* **39,** 467–481.
51. Thomas, R. M., Baici, A., Werder, M., Schulthess, G. & Hauser, H. (2002) *Biochemistry* **41,** 1591–1601.
52. Sun, K. & Mauzerall, D. (1996) *Proc. Natl. Acad. Sci. USA* **93,** 10758–10762.
53. van Rotterdam, B. J., Westerhoff, H. V., Visschers, R. W., Bloch, D. A., Hellingwerf, K. J., Jones, M. R. & Crielaard, W. (2001) *Eur. J. Biochem.* **268,** 958–970.
54. Kamp, F., Hamilton, J. A. & Westerhoff, H. V. (1993) *Biochemistry* **32,** 11074–11086.
55. Eisenberg, M., Gresalfi, T., Riccio, T. & McLaughlin, S. (1979) *Biochemistry* **18,** 5213–5223.
56. Marsh, D. (1993) in *Biomembranes: Physical Aspects*, ed. Shinitzky, M. (VCH, New York), pp. 1–28.
57. Kraayenhof, R., Sterk, G. J., Wong Fong Sang, H. W., Krab, K. & Epand, R. M. (1996) *Biochim. Biophys. Acta* **1282,** 293–302.
58. Molyneux, P., Rhodes, C. T. & Swarbrick, J. (1965) *Trans. Faraday Soc.* **61,** 1043–1052.
59. Tanford, C. (1980) *The Hydrophobic Effect: Formation of Micelles and Biological Membranes* (Wiley, New York).
60. Whitmarsh, J. & Govindjee. (1999) in *Concepts in Photobiology: Photosynthesis and Photomorphogenesis*, eds. Singhal, G. S., Renger, G., Irrgang, K.-D., Sopory, S. & Govindjee (Narosa Publishers/Kluwer Academic Publishers, New Delhi), pp. 11–51.
61. Hope, M. J. & Cullis, P. R. (1987) *J. Biol. Chem.* **262,** 4360–4366.
62. Eastman, S. J., Wilschut, J., Cullis, P. R. & Hope, M. J. (1989) *Biochim. Biophys. Acta* **981,** 178–184.